

S12-33  
160526  
P-12

N93-27738

## Superlattice Barrier Varactors\*

C. Raman, J. P. Sun, W. L. Chen, G. Munns,  
J. East and G. Haddad  
Solid State Electronics Laboratory  
University of Michigan, Ann Arbor, Michigan

### Abstract

SBV (Single Barrier Varactor) diodes have been proposed as alternatives to Schottky barrier diodes for harmonic multiplier applications. However these show a higher current than expected. The excess current is due to X valley transport in the barrier. We will present experimental results showing that the use of a superlattice barrier and doping spikes in the GaAs depletion regions on either side of the barrier can reduce the excess current and improve the control of the capacitance vs. voltage characteristic.

The experimental results consist of data taken from two types of device structures. The first test structure was used to study the performance of AlAs/GaAs superlattice barriers. The wafer was fabricated into 90 micron diameter mesa diodes and the resulting current vs. voltage characteristics were measured. A 10 period superlattice structure with a total thickness of approximately 400 Å worked well as an electron barrier. The structure had a current density of about one A/cm<sup>2</sup> at one volt at room temperature. The capacitance variation of these structures was small because of the design of the GaAs cladding layers. The second test structure was used to study cladding layer designs. These wafers were InGaAs and InAlAs layers lattice matched to an InP substrate. The layers have n<sup>+</sup> doping spikes near the barrier to increase the zero bias capacitance and control the shape of the capacitance vs. voltage characteristic. These structures have a capacitance ratio of 5:1 and an abrupt change from maximum to minimum capacitance. The measurements were made at 80 K. Based on the information obtained from these two structures, we have designed a structure that combines the low current density barrier with the improved cladding layers. The capacitance and current-voltage characteristics from this structure are presented.

---

\*This work was supported by the Center for Space Terahertz Technology under NASA Contract No. NAGW-1334 and by the URI-ARO Program Contract No. DAAL03-87-K-0007.

## Introduction

Varactor diodes are an important component of harmonic multipliers operating above 100 GHz. These multipliers are the primary source of power in the submillimeter wave frequency range, where the diode predominantly used is a Schottky barrier device. However, a multiplier based on Schottky diodes suffers certain disadvantages. The circuit is complex, with higher order conversion requiring matching at all frequencies—the input, the output, as well as idler frequencies. The varactor must also be biased to increase the voltage swing and prevent current flow over the barrier in the forward direction. These problems can be overcome by using heterojunction based varactor structures. Implementation of such novel diode structures is motivated by the symmetry of their capacitance vs. voltage characteristic which permits odd harmonic conversion without the added complexity of even harmonic idlers and bias circuitry.

### The Single Barrier Varactor

One possible structure is the single barrier varactor, shown in Figure 1a. The corresponding energy band diagrams under thermal equilibrium and bias are shown in 1b and 1c. The analogue of the metal-semiconductor electron energy barrier found in the Schottky varactor diode is the conduction band offset between the GaAs region and the wider bandgap  $\text{Al}_x\text{Ga}_{1-x}\text{As}$  layer. This energy barrier acts to inhibit electron transport through the structure and ideally should be as large as possible for the device impedance to be purely reactive. When one side is biased relative to the other, the GaAs region on the anode side is depleted of electrons and becomes positively charged, similar to the semiconductor region of a Schottky varactor under reverse bias. Electrons accumulate on the cathode side of the structure, forming a charge separation across the  $\text{Al}_x\text{Ga}_{1-x}\text{As}$  region. The relationship between the stored charge and the applied voltage is non-linear, resulting in a non-constant device capacitance. Moreover, since the structure is symmetric, reversing the sign of the applied voltage merely interchanges the roles of depletion and accumulation regions and does not affect the device capacitance. Therefore the capacitance-voltage characteristic has even symmetry. Early attempts at implementing such varactors were limited in efficiency by high leakage current densities<sup>1</sup>. Details of the leakage current analysis are described elsewhere in these proceedings<sup>2</sup>.

By replacing the single heterostructure by a superlattice barrier, we propose to reduce the carrier transport through the device by increasing the effective barrier height seen

---

<sup>1</sup>Anders Rydberg, Hans Gronqvist, and Erik Kollberg, *Millimeter and Sub-Millimeter Wave Multipliers Using Quantum Barrier Varactor (QBV) Diodes*, IEEE Electron Device Letters, Vol. 11, No. 9, Sept. 1990, pp. 373-375.

<sup>2</sup>H. Hjelmgren, J. East and E. Kollberg, "Thermionic Emission Current in a Single Barrier Varactor," these proceedings.

by an electron. A doping profile modification can improve the capacitance vs. voltage characteristic; however, a trade-off is seen between maintaining a high barrier height and a good C-V profile.

## The Superlattice Barrier Varactor

Although the SBV presents a symmetric C-V characteristic, its efficiency is degraded due to the high leakage current associated with the device because a purely reactive multiplier is more efficient than a resistive one. The true thermionic emission energy barrier seen by an electron in the GaAs regions is not the  $\Gamma$  to  $\Gamma$  energy level offset but the considerably lower  $\Gamma$  to X energy level difference, as seen in Figure 2a. By means of a scattering process an electron incident on the barrier can pass through the  $\text{Al}_x\text{Ga}_{1-x}\text{As}$  region into the X valley of the barrier material. Thermionic emission over this X level requires less kinetic energy than emission over the  $\Gamma$  level and consequently a smaller bias voltage is needed to turn on the current.

The X valley transport can be suppressed by replacing the single heterojunction by a series of barriers interspersed with quantum wells, i.e., a superlattice. Such a superlattice appears in Figure 2b. The well regions are thin, resulting in quantum mechanical confinement. The energy mini-bands are shifted upward considerably with respect to the  $\Gamma$  point in bulk GaAs. A simple calculation indicates that the energy increase can be on the order of an electron volt. Unlike the SBV, there is no longer a continuous X valley current path since the well energies are higher than the X levels. The superlattice structure achieves a larger effective barrier than that of the SBV and suppresses the leakage current.

A thin, highly doped layer between the superlattice and each adjacent  $\text{N}^-$  region can be used to modify the capacitance. The so-called  $\delta$ -doped regions (see Figure 3) are thin and contain a large amount of charge so that at zero bias they remain mostly undepleted. Flat band effects are minimized and the zero bias capacitance is increased. Varying the bias slightly causes almost no change in the depletion width and the capacitance remains constant. However, beyond a threshold voltage, the entire  $\delta$  region becomes depleted and the lightly doped  $\text{N}^-$  region begins to deplete rapidly, causing a sharp drop in the capacitance from its zero bias value.

## Advantages and Disadvantages

In designing superlattice varactors, two material systems were considered: GaAs/AlAs and InGaAs/InAlAs lattice matched to InP. Structure I, seen in Figure 4, shows a 10 period,  $20 \text{ \AA} / 20 \text{ \AA}$  GaAs/AlAs superlattice barrier varactor chosen for examination of the barrier properties. The MBE grown wafer was processed on the front side by photolithography. Contacts were made to the front and back by evaporating a Ni/Ge/Au/Ti/Au

sequence and annealing at 405 degrees Celsius. Mesa diameters of 5 to 90  $\mu\text{m}$  were then chemically etched. The measured room temperature I-V curve in Figure 5 demonstrates the effectiveness of the superlattice in keeping the current to a minimum. At a bias of 1 volt the current density is about 1 A/cm<sup>2</sup>, compared with about 150 A/cm<sup>2</sup> for the single barrier varactor. However, the ratio of maximum to minimum capacitance is insufficient for any significant harmonic conversion.

The second structure, a 40 Å / 40 Å InGaAs/InAlAs superlattice, was designed with doping spikes added, as outlined in Figure 6a. Figure 6b shows the C-V data, taken at 80 K to reduce the parallel conduction current<sup>3</sup>. A close agreement is observed with the capacitance characteristic predicted by a self-consistent quantum mechanical and Poisson solution for the charge and potential distribution throughout the superlattice varactor. When a voltage of approximately 0.2 volts is applied, the capacitance drops sharply to about one-fifth of its zero bias value, corroborating the theoretical expectation. Thus doping profile modifications allow good control of the capacitance-voltage characteristic.

The final structure utilized the low leakage properties of the GaAs/AlAs superlattice and incorporated the doping modifications that had been tested in the InGaAs/InAlAs system. In structure III the same superlattice as Structure I (with one well layer removed from the end for symmetry) was grown on a new varactor wafer which incorporated a doping spike of sheet density  $1 \times 10^{12} \text{ cm}^{-2}$  and a more lightly doped N<sup>-</sup> region than the previous GaAs/AlAs wafer. Figures 7 and 8 present the room temperature I-V and C-V data from 90 micron diameter mesas fabricated on this wafer. Compared with structure I, the leakage current density has increased. This current degradation can be attributed to the following mechanism: the effective electron thermionic emission barrier is reduced by band bending at the barrier edge due to the high electron density in the doping spike. The capacitance and parallel device conductance were simultaneously measured on a HP4275A LCR meter, where the bias was varied until the conductance exceeded the measurement capability of the machine. As seen in Figure 8, the C-V profile exhibits a swing ratio of close to 4. However, the zero bias capacitance was larger than the value predicted by the quantum mechanical analysis by about a factor of 2. The reason for this is not clearly understood at the present time.

Despite the fact that the current levels in the final structure were higher than expected, the superlattice varactor represents improvement over the single barrier varactor. Figure 9 compares the current densities for the two devices at low and high voltages and temperatures. For operation at low temperature or for small voltages the superlattice barrier fares better than the SBV.

---

<sup>3</sup>J. P. Sun, W. L. Chen, J. East and G. Haddad, *C-V Characteristics of Quantum Well Varactors*, Proceedings of the 1991 International Semiconductor Devices Research Symposium.

## Conclusions

We have demonstrated a superlattice barrier varactor in the GaAs/AlAs system which promises to be useful in odd harmonic generation due to its reduced leakage properties when compared with the SBV. Moreover, modification of the capacitance by means of an appropriate doping profile has been demonstrated in the InGaAs/InAlAs material system. A compromise appears, however, between minimizing leakage current levels in the device and achieving a large maximum to minimum capacitance swing ratio. We hope to begin RF testing of the superlattice barrier varactors in the near future.

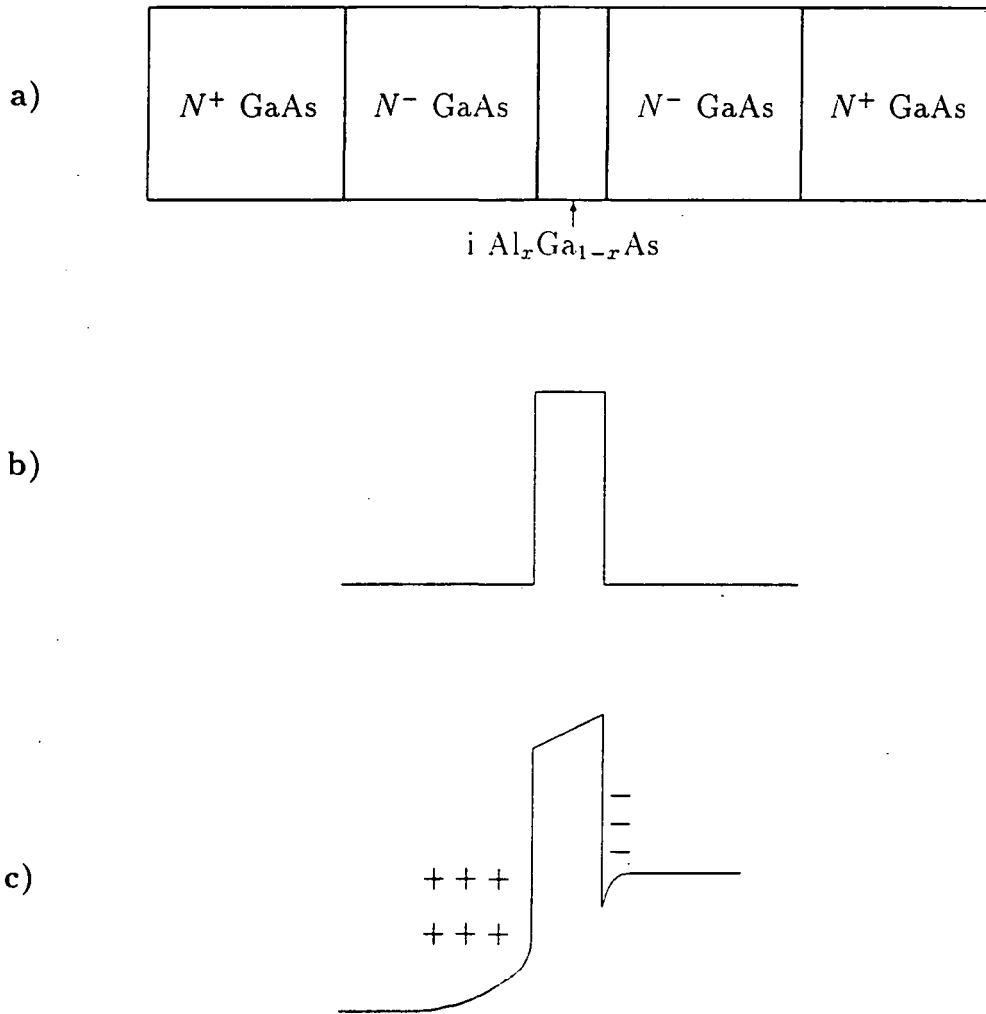
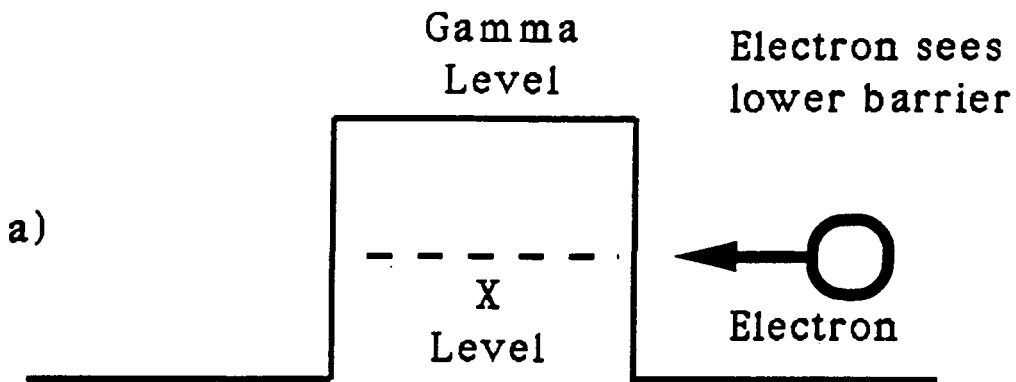


FIGURE (1): (a) Single Barrier Varactor , (b) band diagram under equilibrium, (c) band diagram under bias.



Confined Gamma Energy Levels  
In The Well Regions

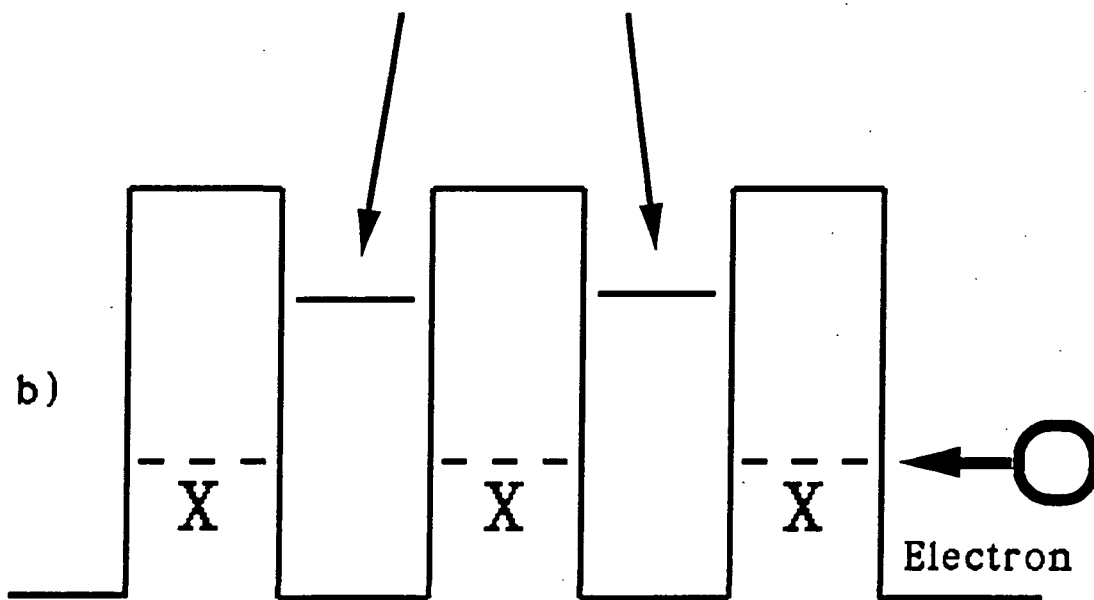


FIGURE (2): (a) X valley transport in Single Barrier Varactor,  
(b) Suppression of X transport by superlattice.

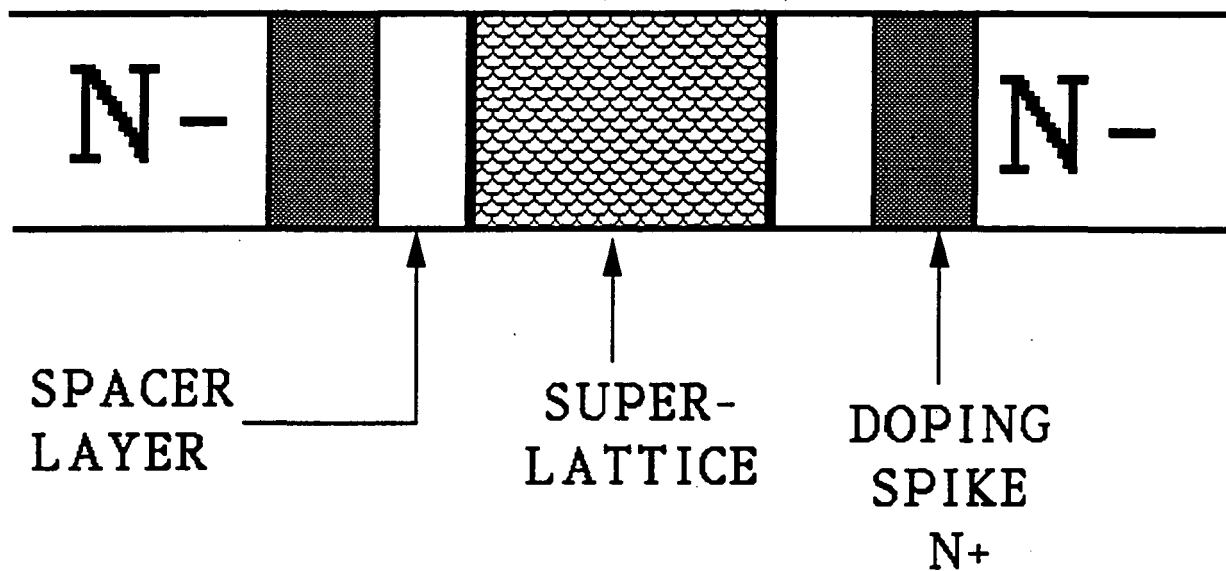


FIGURE (3): Superlattice with doping spikes

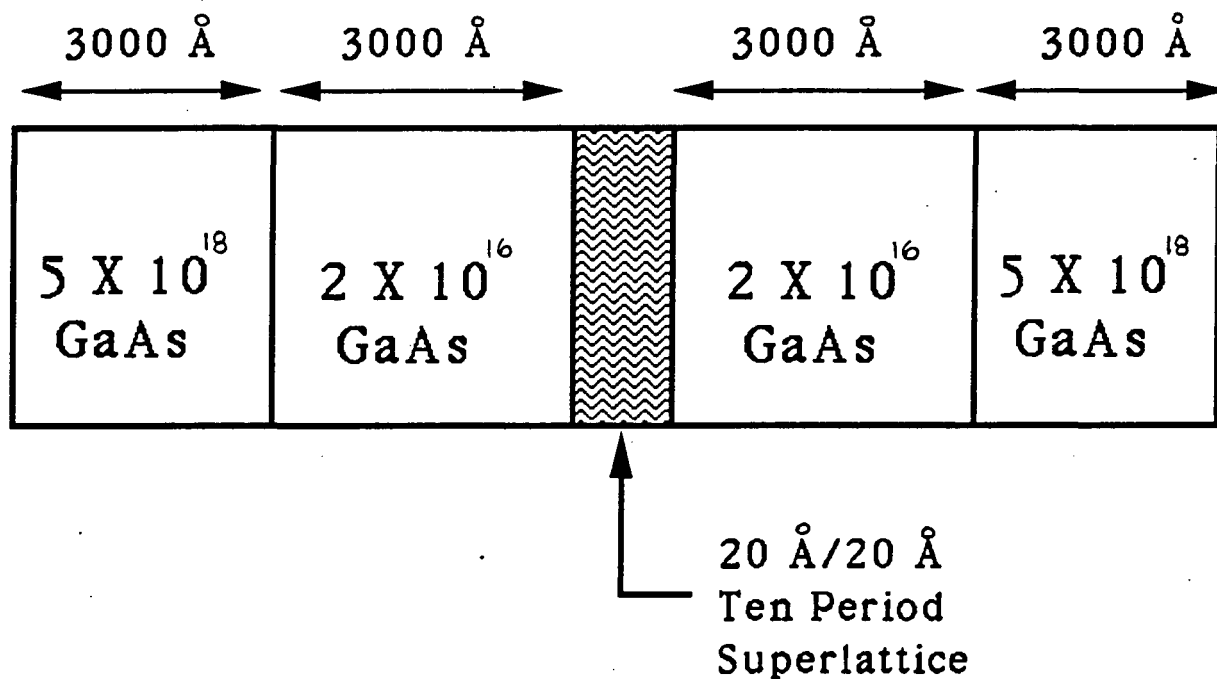


FIGURE (4): Structure I: GaAs/AlAs superlattice varactor



+

\*\*\*\*\* GRAPHICS PLOT \*\*\*\*\*  
SL I-V 90μ DIAM.

IF  
(uA)

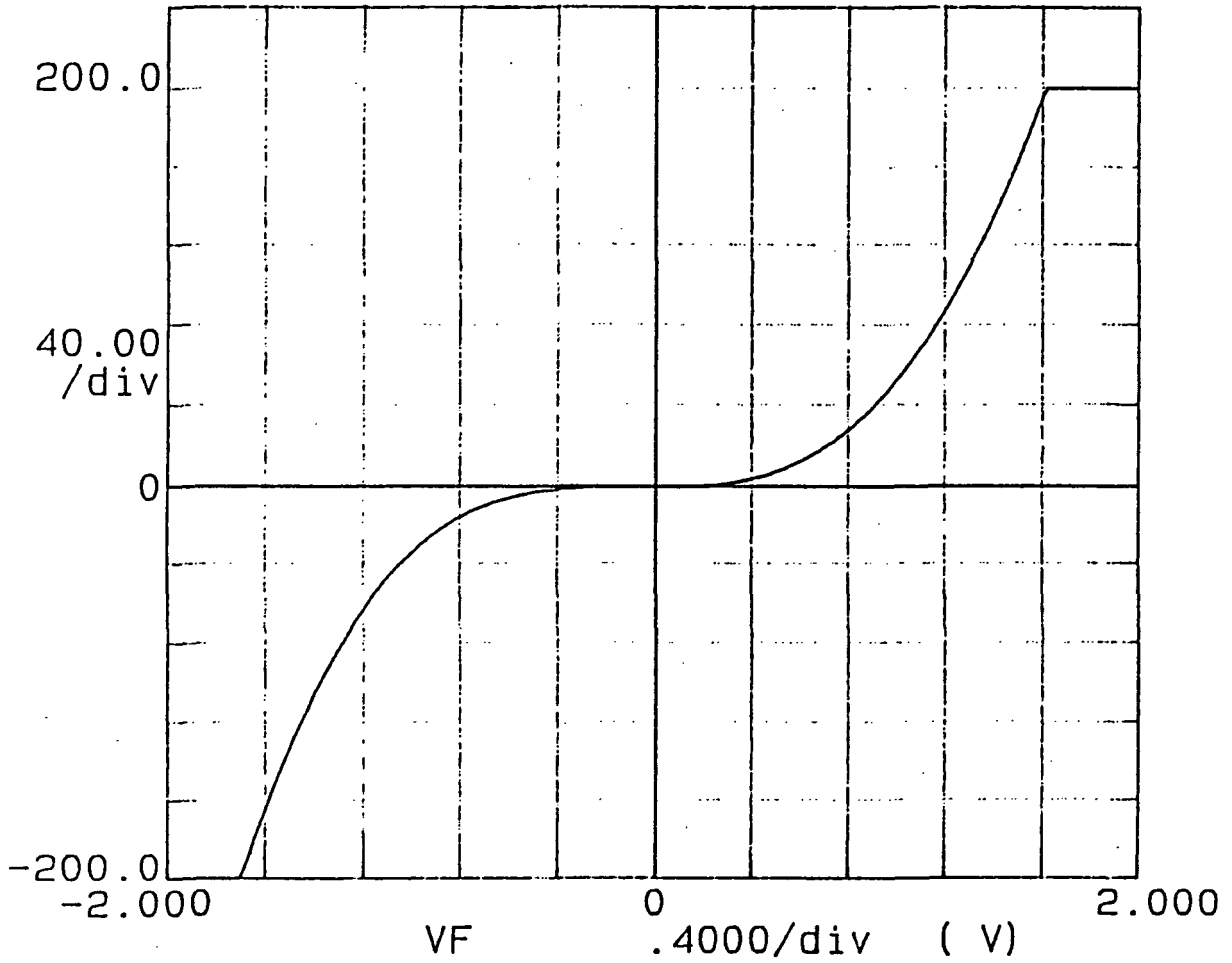


FIGURE (5): Structure I: I-V characteristic

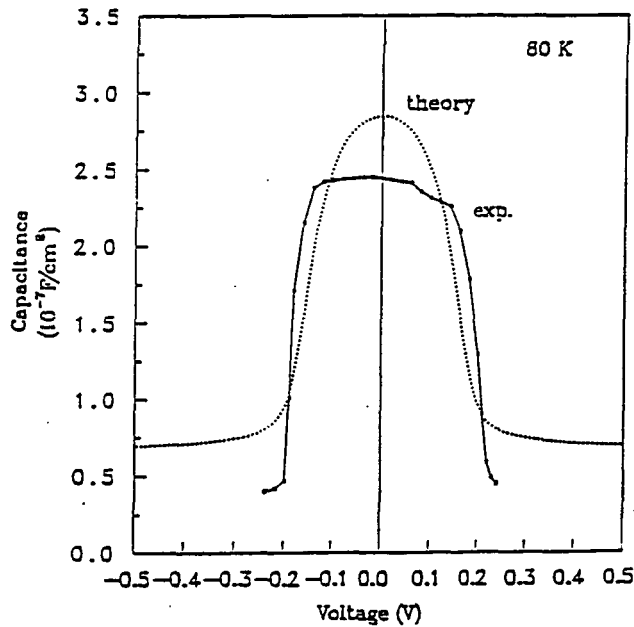
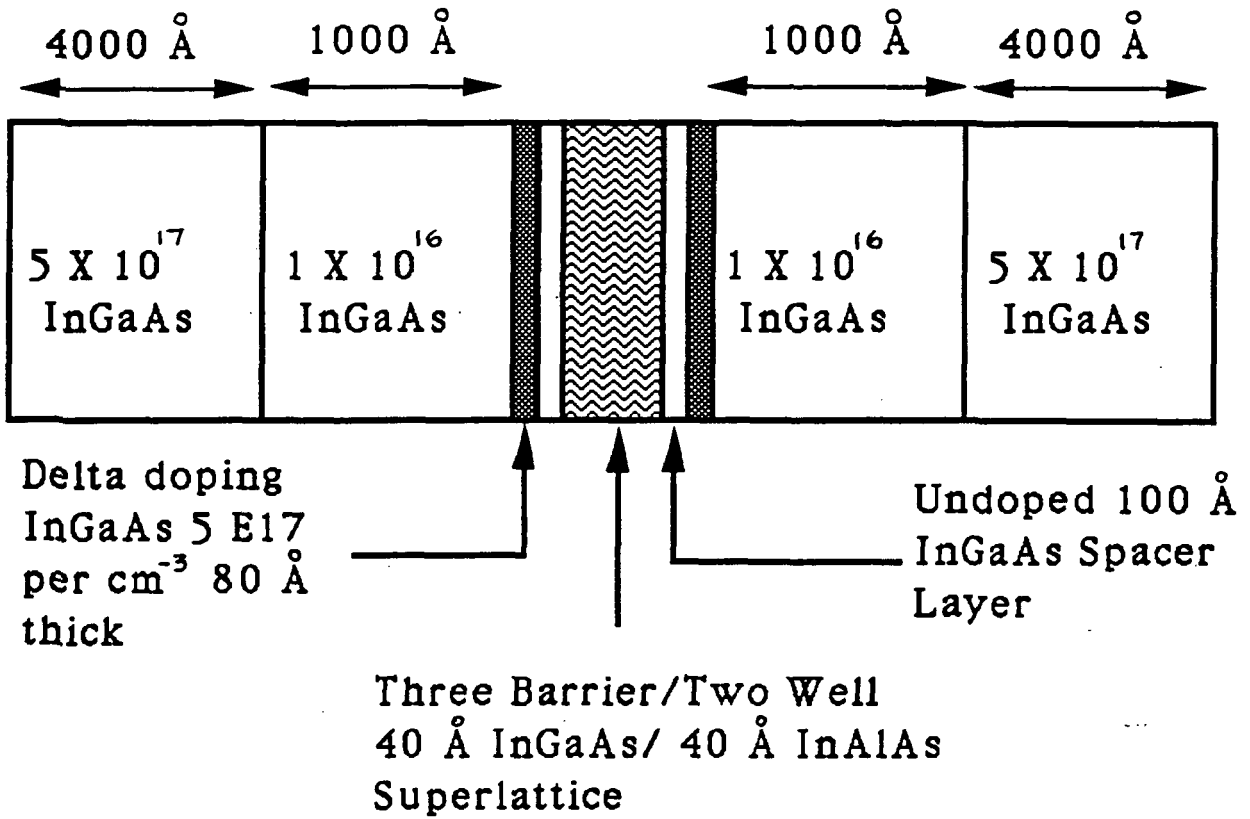


FIGURE (6): (a) Structure II: InGaAs/InAlAs superlattice varactor with doping spikes, (b) Structure II: C-V characteristic

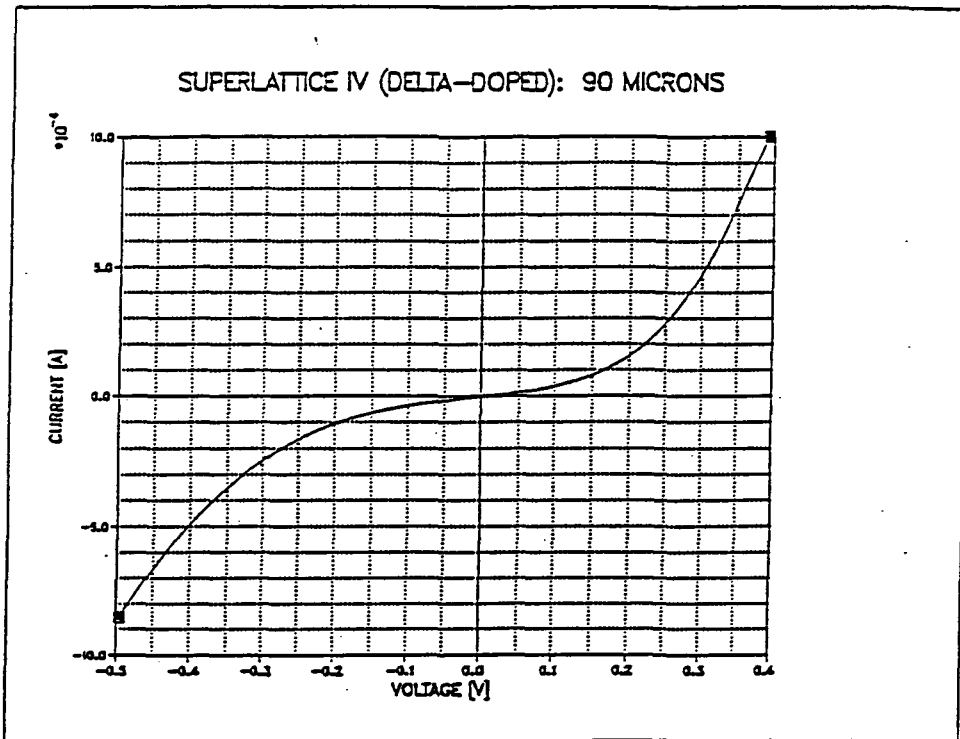


FIGURE (7): Structure III: I-V characteristic

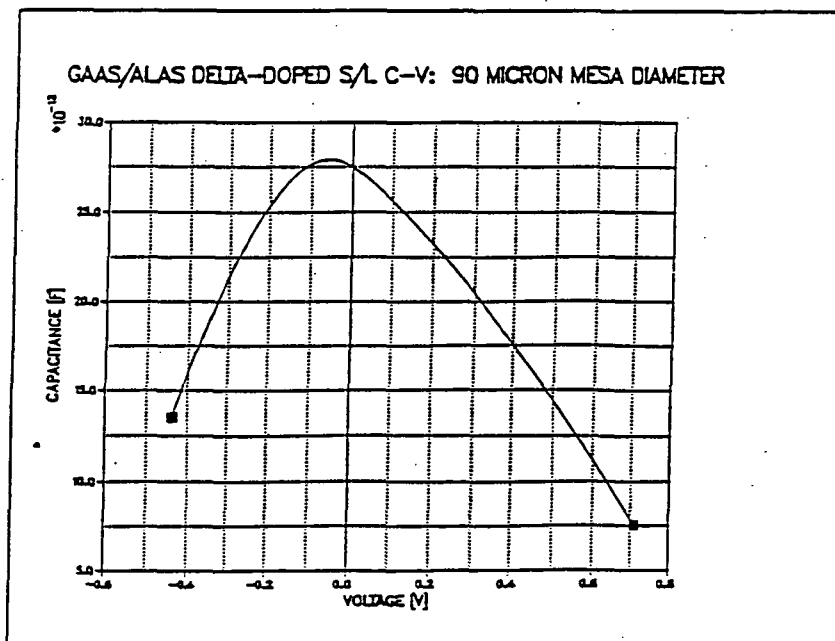


FIGURE (8): Structure III: C-V characteristic

J (Amps/sqcm)

	At V = 0.1 volts	At V = 0.4 volts
SBV	1.1 @ 300 K 0.2 @ 100 K	9.4 @ 300 K 1.8 @ 100 K
AlAs/ GaAs S/L	0.7 @ 294 K negligible @ 90 K	16.5 @ 294 K 0.2 @ 90 K

FIGURE (9): Comparison of improvements